

Degasification system selection for US longwall mines using an expert classification system

C. Özgen Karacan *

National Institute for Occupational Safety and Health, Pittsburgh Research Laboratory, Pittsburgh, PA 15236, USA

A B S T R A C T

Methane emissions from the active face areas and from the fractured formations overlying the mined coalbed can affect safety and productivity in longwall mines. Since ventilation alone may not be sufficient to control the methane levels on a longwall operation, gob vent boreholes (GVB), horizontal and vertical drainage boreholes, and their combinations are drilled and used as supplementary methane control measures in many mines. However, in most cases, the types of degasification wellbores chosen are decided based on previous experiences without analyzing the different factors that may affect this decision.

This study describes the development of an expert classification system used as a decision tool. It was built using a multilayer perceptron (MLP) type artificial neural network (ANN) structure. The ANN was trained using different geographical locations, longwall operation parameters, and coalbed characteristics as input and was tested to classify the output into four different selections, which are actual degasification designs that US longwall mines utilize. The ANN network selected no degasification, GVB, horizontal and GVB, and horizontal, vertical and GVB options with high accuracy. The results suggest that the model can be used as a decision tool for degasification system selection using site- and mine-specific conditions. Such a model can also be used as a screening tool to decide which degasification design should be investigated in detail with more complex numerical techniques.

1. Introduction

Methane emissions can adversely affect both the safety and the productivity of underground coal mines. Generally, it is economically feasible to handle specific emissions (total gas emission per unit amount of coal mined) up to 1000 ft³/ton (28.3 m³/ton) with a well-designed ventilation system. At higher specific emission rates, however, it is difficult to stay within statutory methane limits using ventilation alone (Thakur, 2006). Thus, supplementary methane control measures, such as degasification of the coalbed, are needed prior to or

during mining. Fig. 1 shows a schematic representation of the longwall environment and the different types of degasification boreholes commonly used in US longwall mines.

During longwall mining, methane emissions can originate from the unmined coalbed adjacent to the development entries (ribs) surrounding the ventilation system (Fig. 1), from the active longwall face and mined coal on the conveyor belts, and from subsided strata (Mucho et al., 2000). Emissions from the face are a combination of the methane emitted from the fresh face on the longwall and from the coal on the conveyer belts. Methane emissions from the face, ribs, and conveyor belt are directly discharged into the mining environment. The methane from the fractured and caved rock in the subsided strata (gob) overlying the extracted panel is a

* Tel.: +1 412 386 4008; fax: +1 412 386 6595.
E-mail address: cok6@cdc.gov

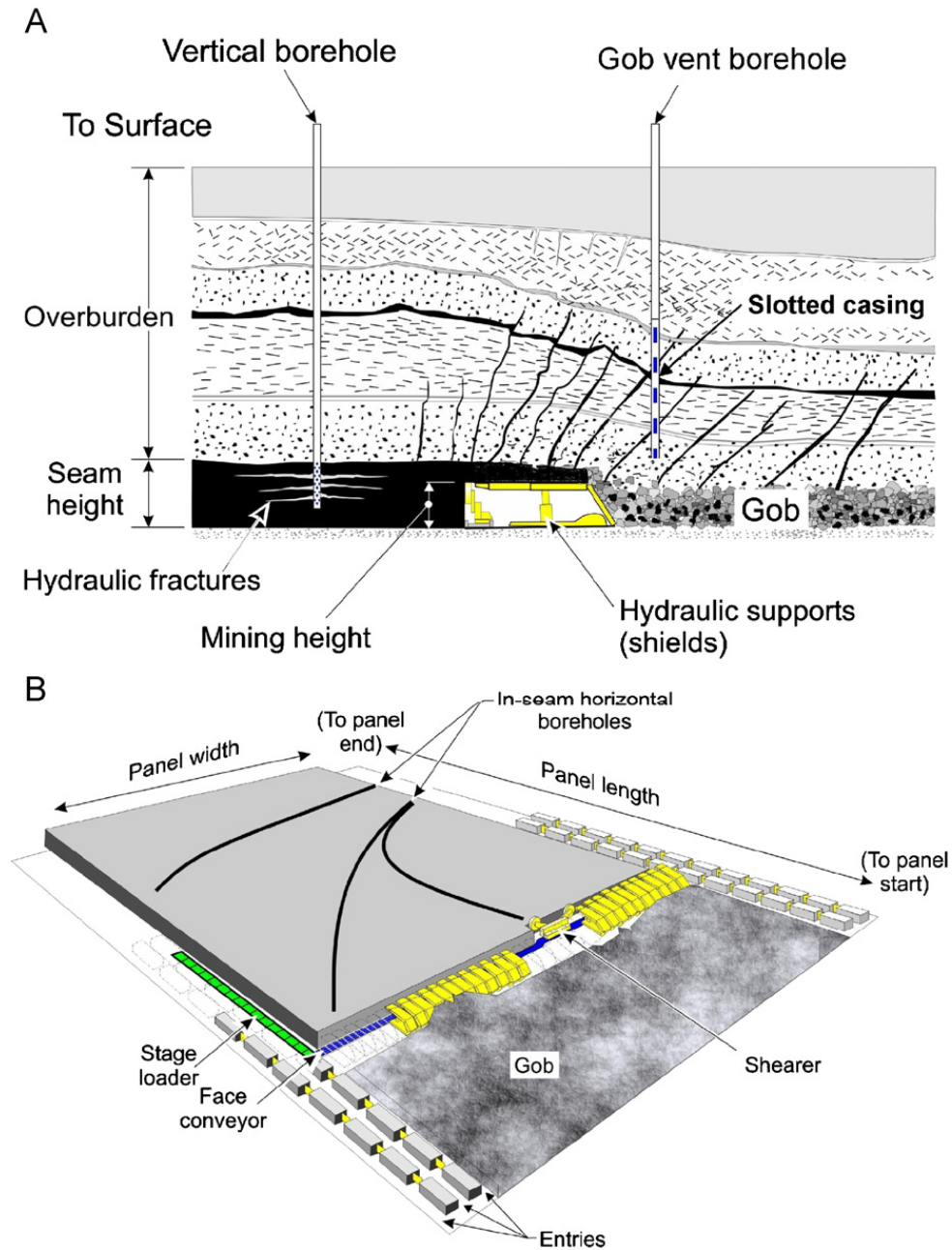


Fig. 1. Schematic representation of longwall mining environment and commonly used degasification borehole types.

big contributor to emissions if overlying strata contain coalbeds and methane-rich sandstones. The emissions from these sources must be controlled effectively, either by the ventilation system or by the degasification boreholes.

Gob vent boreholes (GVB) are commonly used to control the methane emissions from the fractured zone and are drilled from the surface to a depth that places them above the caved zone so that they do not directly interact with the ventilation system (Fig. 1A). The bottom section of the pipe is slotted and placed adjacent to the expected gas production zone. These ventholes generally become productive after the mining-induced fractures propagate under the well (Diamond, 1994; Karacan et al., 2007b). They are equipped with exhausters to capture gas from long distances and reduce methane migration from the fractured zone into the mine.

The most commonly applied methane control technique, especially in high in-place gas content coalbeds, is drilling drainage boreholes into the panel area prior to longwall mining to reduce the methane content of the coalbed and to reduce face emissions during mining. These boreholes can be vertical boreholes drilled from the surface or in-seam horizontal boreholes (Fig. 1A and B) drilled from the gateroad entries (Diamond, 1994; Noack, 1998; Karacan et al., 2007a; Karacan, 2008). In-seam horizontal methane drainage boreholes are usually completed open-hole and they are logistically difficult to drill due to the limited work space. Vertical methane drainage boreholes on the other hand have the distinct advantage of not being conducted in the restrictive underground environment. They are mostly suited for highly gassy, deep, low-permeability coal seams where

it takes a long time prior to mining to adequately degasify the coalbed (Thakur, 2006). However, the drainage area of vertical wells is limited compared to that of horizontal boreholes. Thus, in most circumstances vertical wells need to be stimulated by hydraulic fracturing (Fig. 1A).

Vertical wells are often used in the San Juan Basin in New Mexico and in the Black Warrior Basin in Alabama since degasification of the coalbeds is started with vertical wells a long time ahead of mining and also since commercial coalbed methane production started in these regions earlier than many other regions. They are also used to degasify coalbeds in the Central Appalachian Basin of Virginia and West Virginia (Diamond, 1994). Although stimulated boreholes have been shown to be effective in draining methane from virgin coalbeds, the technology has not been universally accepted by the US mining industry due to concerns that hydraulic fracturing might adversely affect the integrity of the weak roof material, especially in the Northern Appalachian Basin.

Despite different drainage methods are used in most US longwall operations, some operations do not use any degasification if the gas emission levels can be effectively controlled with ventilation. In most cases, a combination of different drainage methods leads to the highest recovery of methane from the coalbed and its overlying strata. The preferred methane recovery method depends on the mining parameters and the gassiness of the coal seam. Table 1 provides a summary of the degasification methods used by US longwall mines and the approximate efficiencies of these methods (EPA, 2005).

1.1. Motivation and objective of the study

Predicting the rate of methane emissions into working areas and the design of an effective degasification system are complex due to the number of factors involved. Modifications to an existing methane drainage system, especially after the methane problem has already become severe, may result in higher costs and may create safety problems. Thus, it may be advantageous to determine the need for and the most effective type of degasification before mining starts by considering the various geological, coalbed, and mining parameters. This type of assessment prior to mine development generally requires both empirical and theoretical approaches.

Table 1

Common degasification systems used and their drainage efficiencies, calculated based on percentage of methane recovered that would otherwise be emitted

| Method | Description | Gas quality | Drainage efficiency | Current use in US coal mines |
|-------------------------|--|---|---------------------|------------------------------|
| Vertical pre-mine wells | Drilled from surface to coalbed months or years in advance of mining | Nearly pure methane | Up to 70% | > 8 mines |
| Gob vent boreholes | Drilled from surface to a pre-determined depth to the top of the coalbed | Methane contaminated with mine air, especially later in production life | Up to 50% | > 17 mines |
| Horizontal boreholes | Drilled from inside the mine to degasify the coalbed and to shield the entries | Nearly pure methane | Up to 50% | > 18 mines |
| Cross-measure boreholes | Drilled from inside the mine to degasify the surrounding strata | Methane, sometimes contaminated with mine air | Up to 20% | Not used widely |

Insight into the selection and configuration of effective methane drainage systems can be gained from reservoir simulations (King and Ertekin, 1989; King et al., 1986; Remner et al., 1986; Brunner et al., 1997; Diamond et al., 1989; Kelafant et al., 1988; Karacan et al., 2007a). However, a comprehensive mine simulator combining mining operation, coalbed reservoir, and methane production parameters does not exist (Diamond, 1994). A technique that can identify the optimal degasification system for a given set of mining and geological parameters could be used as a screening tool prior to employing other numerical modeling techniques.

Artificial neural networks (ANNs) may fill the gap where model-based diagnosis systems are not present or are not adequate for making fast but reliable decisions. ANNs are typically used for complex problems that are difficult to describe mathematically. The pattern classification application can be regarded as a specific case of function approximation where the mapping is done from the input space to a finite number of output classes (Hong et al., 2003). Classification problems using ANNs have been successfully applied to other fields of science (An et al., 1995; Brown et al., 1998; Chen et al., 2002; Kılıç et al., 2007).

The aim of this paper is to develop an ANN-based expert classification system to identify the need and the type of degasification system for a longwall operation. The ANN model was built using a multilayer perceptron (MLP) approach to map the inputs to four different degasification options (N: none; G: gob vent borehole; HG: horizontal boreholes and gob vent boreholes; VH: vertical, horizontal boreholes and gob vent boreholes). The model was developed using a database built on the operational, coalbed, and geologic parameters and on the degasification practices of US longwall mines. Such a model can be used as a decision tool for selection of a degasification system and can also be used as a screening model before designing degasification systems using more detailed numerical modeling methods.

2. Description and analysis of database

2.1. Sources of input data

In developing the database, information on 63 longwall mines in 10 states operating from 1985 to 2005 was collected from various data sources. These sources

provided gas contents of the mined coalbeds, annual coal productions and emissions, longwall mining operation parameters, mine characteristics, as well as the type of degasification system utilized.

Gas contents of the mined coalbeds, based on their geographical location and the overburden depths of the mines, were compiled from a report published by Diamond et al. (1986). This publication reports the gas content data for approximately 1500 coal samples from more than 250 coalbeds in 17 states. The components of total gas content (lost, desorbed, and residual gas contents) were reported along with sample location (state and county), sample depth, coalbed name, coal rank, and ash content for each sample. The lost gas was determined by a graphical method and estimated how much gas was lost during core recovery. Desorbed gas was determined using the direct method determination of gas content (Diamond and Schatzel, 1998), and residual gas was determined after crushing the coal samples with a ball mill. The total gas content was the sum of all components.

Annual coal productions, ventilation emission data, and degasification systems utilized by the operations were reported in US Environmental Protection Agency (EPA) reports (1994, 2005). These reports listed geographical data, availability of degasification systems, type of degasification system, sulfur content and calorific value of mined coals, annual coal productions, and emissions from ventilation systems.

Mining parameters and mine characteristics are important for degasification system selection since they can affect methane emissions. The annual data representing these two groups were compiled from 1985 to 2005 issues of Coal Age magazine, which annually publishes longwall census data. The tabulated data for each operating mine in the corresponding year includes seam height, cutting height, cutting depth, overburden thickness, longwall panel width, longwall panel length, number of gateroad entries, face conveyor speed, and stage loader speed.

Tables 2 and 3 show the names and the number of longwall mines operating in each state and the variables compiled from the data sources, respectively. After evaluation of all data, the database consisted of 538 data entries with 24 variables spanning a 20-year period. Of

these 538 data entries, 93 (17%) had G-type degasification method, 136 (25%) had HG-type system, 153 (28%) had VHG-type system, and 156 (30%) did not have any degasification system installed (N type).

2.2. Discussion of database parameters for their potential effects on selection of degasification systems

This section summarizes the possible effects of the variables presented in Table 3 on ventilation emissions. Some of these variables are shown in Fig. 1, which also provides schematic representation of various degasification borehole designs. Fig. 1B shows the graphical representation of a panel surrounded by a three-entry gateroad system, the gob behind the shields, the face area, the transportation systems, and an unmined section of the coal seam. Fig. 1A is a vertical cross-section along the panel length in Fig. 1A. This figure shows the overlying strata, hydraulic shields, longwall face area, and caving and fracturing of the overlying strata.

2.2.1. Overburden, coal seam properties (gas content, rank, seam height), and emission from ventilation system

Depth of the mined coal seam, or the overburden (Fig. 1A), has two potential impacts on the selection of an

Table 3

Variables and their units in database for each mine compiled from different sources

| Variable | Unit | Variable | Unit |
|-----------------------------|-----------|----------------------------|--------------|
| State | | Ash content | % |
| Basin | | Coal production | mill. t/year |
| County | | Seam height | Inch |
| City | | Cut height | Inch |
| Ventilation emission | MMscf/day | Panel width | ft |
| Mined coalbed | | Panel length | ft |
| Sulphur amount | % | Overburden | ft |
| Coal calorific value | Btu/lb | Number of entries | |
| Lost+desorbed gas | scf/ton | Cut depth | Inch |
| Residual gas | scf/ton | Face conveyor speed | ft/min |
| Total gas | scf/ton | Stage loader speed | ft/min |
| Rank | | Year | |

Variables in bold are not included into PCA.

Table 2

Number of mines and mine names in each state included into database for modeling

| State | | No. of mines | Mine names |
|---------------|----|--------------|--|
| Alabama | AL | 8 | Blue Creek No. 3, Blue Creek No. 4, Blue Creek No. 5, Blue Creek No. 7, North River, Mary Lee, Oak Grove, Shoal Creek |
| Colorado | CO | 4 | Deserado, Dutch Creek, Golden Eagle, West Elk |
| Illinois | IL | 7 | Galatia, Old Ben 24, Old Ben 25, Old Ben 26, Orient No. 6, Monterey No. 1, Rend Lake |
| Kentucky | KY | 4 | Wolf Creek No. 4, Wheatcroft No. 9, Camp No. 11, Baker |
| Maryland | MD | 1 | Mettiki |
| Ohio | OH | 4 | Meigs No. 2, Meigs No. 31, Powhatan No. 4, Powhatan No. 6 |
| Pennsylvania | PA | 10 | Bailey, Eighty Four, Enlow Fork, Maple Creek, Cambria, Cumberland, Warwick, Homer City, Dilworth, Emerald |
| Utah | UT | 4 | Aberdeen, Sunnyside No. 1, Dugout Canyon, West Ridge |
| Virginia | VA | 7 | Buchanan, V.P. No. 8, V.P. No. 1, V.P. No. 6, V.P. No. 5, V.P. No. 3, McClure No. 1 |
| West Virginia | WV | 14 | Blacksville No. 2, Federal No. 2, Loveridge No. 22, McElroy, Pinnacle No. 50, Robinson Run No. 95, Ireland, Osage No. 3, Shoemaker, Windsor, Shawnee, Arkwright, Blacksville No. 1, Humphrey No. 7 |

effective degasification system. The first one is its effect on methane content. For coals of the same rank, gas content generally increases with increasing depth (Kim, 1977). Increasing gas content usually increases the gas emissions in the mine and may prompt the use of vertical or horizontal methane drainage boreholes for degasification of the coalbed before or during mining. Fig. 2 shows the change in total gas content (for various rank coals) with overburden depth for the reported 1500 samples in Diamond et al. (1986).

The second impact of overburden depth is its effect on the disturbances created in the overlying strata. If panel width is greater than the overburden, the panel is called “supercritical” (Mucho et al., 2000), and thus the caving will be more complete after mining compared to a situation where the panel width is less than overburden depth. This situation may potentially affect the methane reservoir and permeability pathways in the overlying strata (Karacan et al., 2005) and may promote reconsideration of some of the design parameters for gob vent boreholes.

Fig. 3 shows the types of degasification systems used in US longwall mines as a function of overburden depth. The graph suggests that overburden depths do not affect the use of a particular degasification system. However, a majority of the mines that do not use any of the degasification systems operate between depths of 200 and 700 ft (61 and 213 m). These are fairly shallow mines and therefore methane emissions likely can be controlled by the ventilation system alone. The majority of the mines that use the VHG system, on the other hand, operate at depths between 500 and 2100 ft (152 and 640 m). Gob vent boreholes, as the sole degasification system, are used by mines that operate at depths between 500 and 1200 ft (152 and 366 m), although there are deeper mines that use only gob vent boreholes for degasification.

Total gas content has three major components: lost gas, desorbed gas, and residual gas. In a mining operation, all

of the components may contribute to emissions and may affect the degasification system choice. The gas content data, when combined with geologic and engineering data, can provide an initial estimate of possible emissions into the mine and an initial selection of a degasification system design to control these emissions (Diamond et al., 1986; Karacan and Diamond, 2006; Noack, 1998). Fig. 4 shows the degasification methods as a function of total gas content of the coalbed. The figure shows that as the coalbed gets gassier, most mines tend to use HG- or VHG-type systems. For instance, the majority of the mines operating in coalbeds with gas contents between 350 and 550 scf/ton (9.9 and 15.6 m³/ton) use a VHG-type system.

Coal rank represents the level of maturation of the coal seam. Most longwalls operate in bituminous coalbeds. The sub-bituminous to low-volatile (LV) bituminous coals usually have high gas contents and permeabilities (Steidl, 1996). Thus, mining coals of this range, particularly medium-volatile (MV) to LV bituminous coals, can

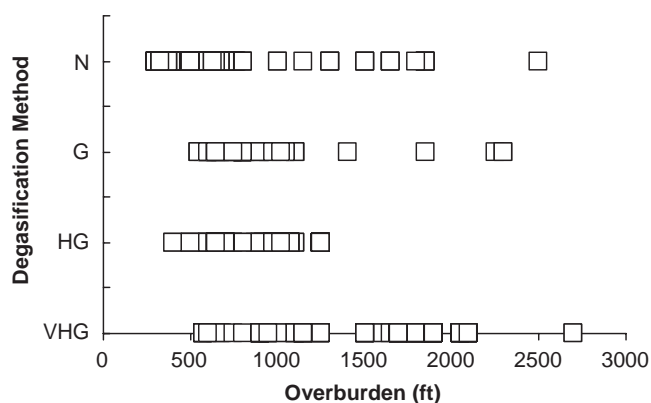


Fig. 3. Types of degasification systems used in US longwall operations as a function of overburden depth (N: none; G: gob vent borehole; HG: horizontal borehole and gob vent borehole; VHG: vertical, horizontal and gob vent borehole).

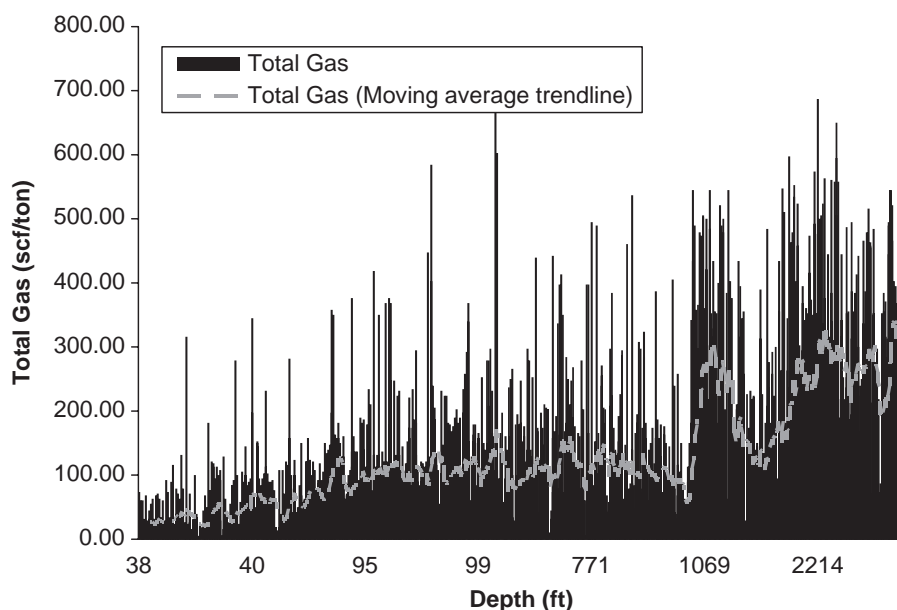


Fig. 2. Total gas contents of the coals reported in Diamond et al. (1986) as a function of core depth.

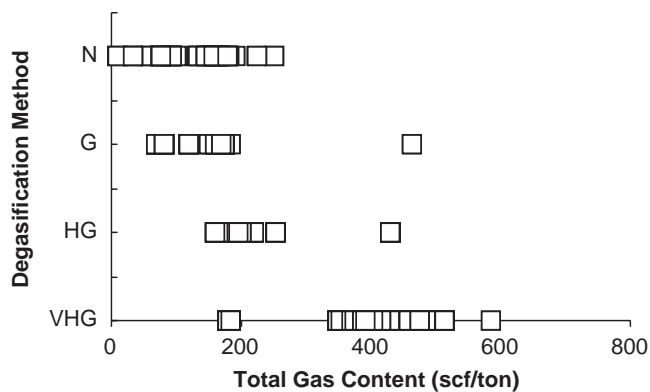


Fig. 4. Types of degasification systems used in US longwall operations as a function of total gas content of coalbed (N: none; G: gob vent borehole; HG: horizontal borehole and gob vent borehole; VHG: vertical, horizontal and gob vent borehole).

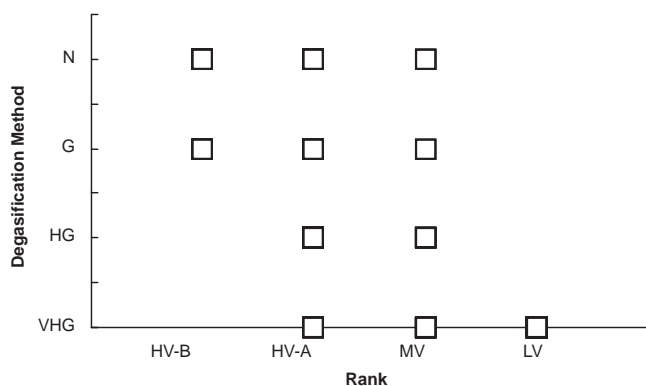


Fig. 5. Types of degasification systems (N: 156, G: 93, HG: 136, VHG: 153) used in US longwall operations as a function of coal rank (HV-A: high-volatile A; HV-B: high-volatile B; MV: medium-volatile; LV: low-volatile).

potentially liberate high amounts of gas into the work environment. Fig. 5 shows the variation of the degasification systems used in longwall mines in the dataset as a function of coal rank. The figure shows that as the rank varies from high-volatile (HV) to MV and LV bituminous, a VHG-type system is preferred.

Seam thickness and mining height (Fig. 1A) impact emissions in two ways. First, thick coal seams have higher face and rib emissions (Karacan, 2008) compared to their thinner counterparts due to increased surface area. Second, the mining height impacts the thickness of the fractured zone in the gob. This situation potentially can result in more gas flowing from the overlying strata into the mine environment. This situation affects gob vent borehole drilling needs and design criteria.

Predicted emissions impact the use of the degasification scheme (Karacan, 2008). Degasification of the coal seam and the fractured strata prior to and during mining are effective ways of controlling methane emissions during mining (Diamond, 1994; Karacan et al., 2007a). Depending on the gassiness of the coal seam and the fractured strata, horizontal boreholes, vertical boreholes, or gob vent boreholes can be used. The number of boreholes, their locations, and their degasification durations may change based on the site-specific factors. Fig. 6

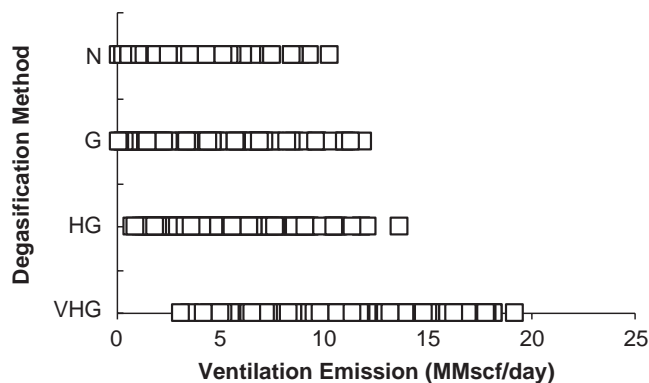


Fig. 6. Types of degasification systems used in US longwall operations as a function of daily methane emission rates from ventilation system (N: none; G: gob vent borehole; HG: horizontal borehole and gob vent borehole; VHG: vertical, horizontal and gob vent borehole).

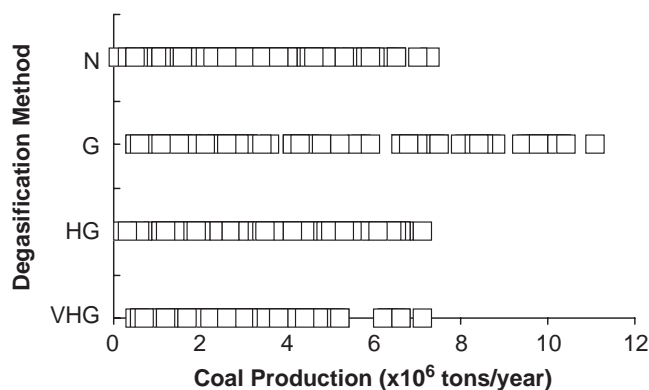


Fig. 7. Types of degasification systems used in US longwall operations as a function of annual coal production (N: none; G: gob vent borehole; HG: horizontal borehole and gob vent borehole; VHG: vertical, horizontal and gob vent borehole).

shows the types of degasification systems used as a function of daily methane emission rates from the ventilation system. This figure shows that the mines with the highest emissions tend to use VHG- and HG-type degasification systems.

2.2.2. Operational, mine design, and coal productivity data

Practical experience has shown that emissions are related to coal production rates. Thus, expected coal production may affect degasification options for specific mine conditions. Fig. 7 shows the type of degasification system as a function of coal productivity. This figure shows that the coal productivity of those mines that use only gob vent boreholes spans a wide range. This may be due to the moderately gassy nature of these operations. Productivity of these mines is followed by those that use HG-type systems. The increasing size of longwall panels (width and length) usually affects coal production and methane emissions due to the exposure of the mining environment to wider faces and to a larger area of fractured strata. If not captured effectively, additional gas emissions from a larger area of fractured formations can enter the mining environment and may create unsafe operating conditions (Karacan et al., 2005). Thus, as the size of the panel increases, the expected increase in

emissions must be controlled by effective degasification methods.

Cutting depth is the slice of coalbed that is mined by the shearer during each pass. In general, greater cutting depth produces more coal per rotation of the cutting drum with an increase in emissions. However, shearer speed and rotational speed of the cutting drum are also important. Thus, cutting depth may not be a determining factor by itself for selecting degasification options.

Gateroad entries (Fig. 1B) surrounding the panels are mainly used for ventilation and transportation pathways. In the US, some of the early longwalls used five-entry gateroads. However, three entries are preferred since this requires less development footage compared to four- or five-entry systems. Four-entry systems are used in coal seams of low height or high gas content, where air flow resistances and air flow requirements are high. Two entries require a special permit and are used in deep mines with a thick layer of strong overlying strata (Peng, 2006). Thus, the number of entries may be an indicator of the gassiness of the mine.

2.2.3. Geographical location (state and basin)

A strong relationship exists between the gas emission rates and the geological factors of a particular site, such as the stratigraphy, the gas contents, and the strengths of the overlying and underlying strata. Pashin (1998) reported, based on the investigations in the Black Warrior Basin and in San Juan Basin, that regional variations in sequence stratigraphy are useful for characterization of coalbed methane reservoirs since they are affected by regional sedimentology and tectonics. Although geographical location is not directly related to the choice of the degasification system, it indirectly identifies the differences between underground stratigraphy and emissions due to local variations in reservoir characteristics. Thus, geographical location may be used to include these parameters in decisions regarding design of the degasification system.

3. Model complexity reduction using principal component analysis (PCA) and evaluation of database variables

In this study, PCA was used for selecting the most appropriate input variables from all the variables presented in Table 3 for developing an ANN-based classification system. Identifying principal components (PCs) and eliminating those that do not contribute to the variance of the data decreases the dimension of the data set, while retaining most of the variance and revealing information on correlations between variables (Grima, 2000).

Before performing PCA, city, county, calorific value (Btu), ash content, sulfur content, face conveyor speed, stage loader speed, coalbed, and year information in Table 3 were eliminated from the analysis, since they either were irrelevant for the purpose or they could be better represented by other variables in the data set. With elimination of these nine variables, Table 3 was reduced to 15 variables. The variables represented by alphanumeric information were designated by numeric information

(such as state) for PCA. For instance, numeric codes of states were used for identification.

Table 4 lists the results of the PCA performed on the remaining 15 variables in Table 3. It can be seen that all variance in the data is represented by 14 PCs. However, approximately 80% of the variance can be represented by the first five PCs. The individual contributions of the remaining 9 PCs are small and their total contribution is only 20% of the total variance. The eigenvalues, which are the proportion by which an eigenvector's magnitude is changed, is also shown in Table 4. Table 4 shows that the largest eigenvalues (strongest correlations in the data set) are also in the first five PCs. Thus, five PCs, whose factor loadings are shown in Table 5, were selected as the PC matrix.

Figs. 8A and B show the correlation circles for the factor loadings of PC1 and PC2 and PC1 and PC3, respectively. These figures show the degree of correlation between variables and the PCs. In these plots, any two variables that are far from the center and close to each other are significantly and positively correlated. On the

Table 4

Eigenvalues and variances explained by principal components extracted using 538 observations of 15 variables shown in Table 3

| PC | Eigenvalue | Variance (%) | Cumulative % |
|----|------------|--------------|--------------|
| 1 | 4.88 | 32.56 | 32.56 |
| 2 | 2.75 | 18.31 | 50.87 |
| 3 | 2.35 | 15.64 | 66.51 |
| 4 | 1.40 | 9.36 | 75.87 |
| 5 | 0.87 | 5.79 | 81.66 |
| 6 | 0.66 | 4.41 | 86.07 |
| 7 | 0.54 | 3.57 | 89.64 |
| 8 | 0.42 | 2.83 | 92.47 |
| 9 | 0.40 | 2.69 | 95.16 |
| 10 | 0.27 | 1.82 | 96.98 |
| 11 | 0.22 | 1.49 | 98.47 |
| 12 | 0.12 | 0.77 | 99.24 |
| 13 | 0.08 | 0.57 | 99.80 |
| 14 | 0.03 | 0.20 | 100.00 |

Table 5

Loadings of variables in principal component matrix for first five principal components

| Variables | PC 1 | PC 2 | PC 3 | PC 4 | PC 5 |
|----------------------|--------|--------|--------|--------|--------|
| Basin | -0.720 | 0.238 | -0.404 | 0.423 | -0.170 |
| State | -0.492 | 0.371 | -0.589 | 0.444 | -0.153 |
| Seam height | 0.244 | 0.095 | 0.693 | 0.581 | 0.132 |
| Cut height | 0.303 | -0.057 | 0.715 | 0.518 | 0.137 |
| Panel width | -0.024 | 0.752 | 0.255 | -0.237 | 0.004 |
| Panel length | -0.339 | 0.627 | 0.118 | -0.355 | 0.034 |
| Overburden | 0.797 | 0.149 | -0.191 | 0.152 | -0.054 |
| Number of entries | 0.338 | -0.026 | -0.535 | -0.015 | 0.675 |
| Cut depth | 0.019 | 0.709 | 0.296 | -0.097 | -0.214 |
| Lost+desorbed gas | 0.896 | 0.192 | -0.178 | 0.102 | -0.240 |
| Residual gas | -0.528 | 0.470 | -0.299 | 0.379 | 0.276 |
| Total gas | 0.837 | 0.305 | -0.253 | 0.190 | -0.195 |
| Rank | 0.865 | 0.223 | -0.332 | -0.016 | -0.051 |
| Coal production | -0.308 | 0.689 | 0.241 | -0.073 | 0.176 |
| Ventilation emission | 0.694 | 0.423 | -0.026 | -0.108 | 0.262 |

other hand, variables on the opposite sides of the center are negatively correlated. Variables close to the center are not represented well by those axes and their information may be hidden in other PCs and in the properties that they represent. Fig. 8A shows that total gas content, rank of the coal, and ventilation emissions are correlated with overburden thickness and that they are significant for the first PC. Likewise, panel length is correlated with coal production and these same variables are significant for the second PC. On the other hand, seam height, cut height, and number of gateroad entries are close to the center, suggesting that their information can be better represented by other PC axes. Fig. 8B is a similar diagram for PC1 and PC3 which shows that total gas content, coal rank, overburden depth, and gas emission data are still

correlated and significant on PC1. Seam and cut (mining) heights show significant correlation with each other and with PC3. On the other hand, the lengths of panel dimensions and coal production get smaller since these variables are significant on PC2, not on PC3.

The factor scores of each observation on each PC can be plotted to investigate the trends and groupings. Figs. 9A and B show a two-dimensional map of the factor scores of each mine on axes PC1 and PC2 and on axes PC1 and PC3, respectively. These plots enable the analyses of the trends and groupings between mines based on the variables they represent on each PC. Figs. 9A shows that there are two major clusters: The cluster on the right side is formed by Virginia and Alabama mines while the one on the left is formed by the mines in the remaining eight states. Virginia and Alabama mines are separated from the others because of the mining depths, gassiness, and the evaluated operation parameters. The scattered data points between these two main clusters are due to these operations having characteristics of the mines in both states. For instance, the data points located on the positive

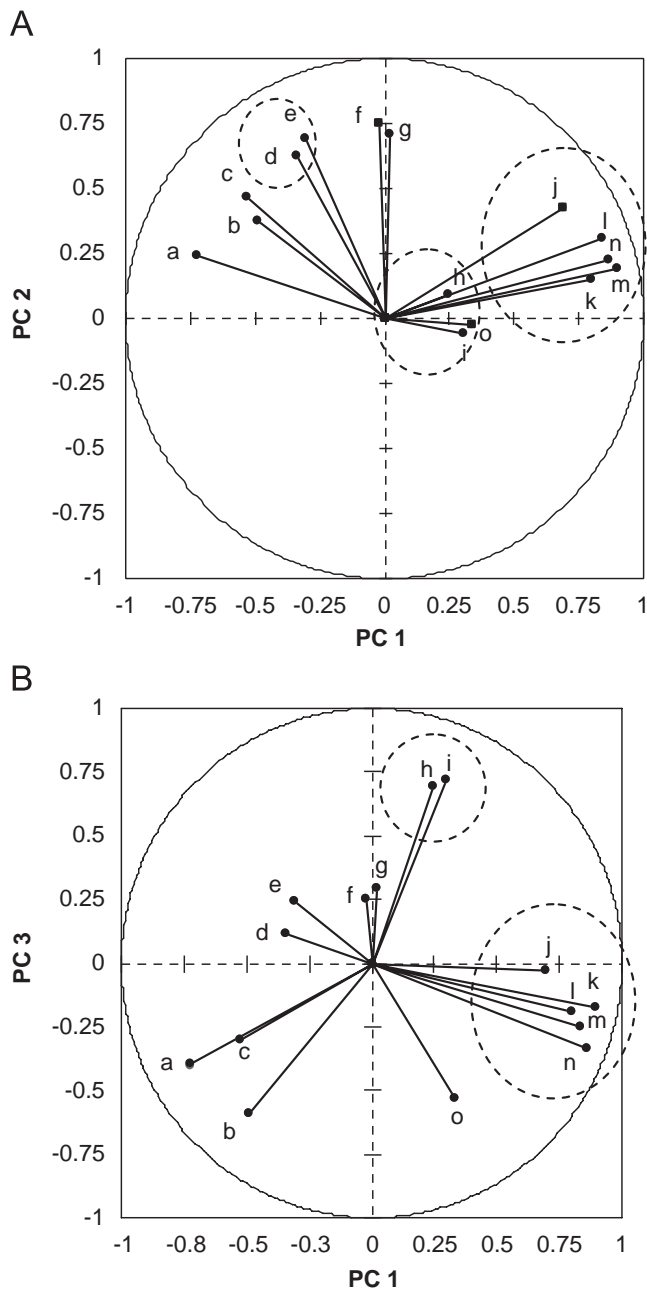


Fig. 8. Correlation circles showing magnitude and directions of variable loadings in PC1-PC2 (8A) and PC1-PC3 (8B).

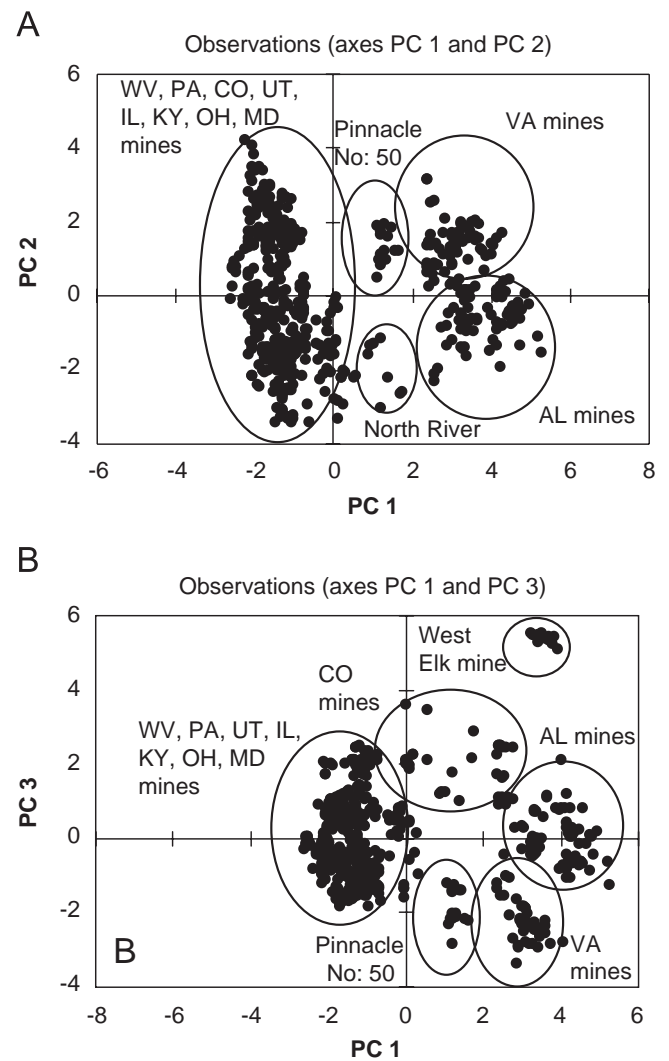


Fig. 9. A two-dimensional distribution of factor scores of each mine on PC1-PC2 (Fig. 9A) and PC1-PC3 (Fig. 9B) determined by PCA. Plot shows groupings of mines based on different characteristics.

side of PC2 belong to Pinnacle No. 50 mine. Although this mine is geographically located in West Virginia, it is operating in the Pocahontas No. 3 coalbed which makes it similar to the Virginia mines operating in this coalbed. Some of the data on the negative side of axis PC2 belong to the North River mine in Alabama, where the overburden (500–600 ft) and gas content of the coalbed are less than those at other Alabama mines.

Fig. 9B shows the factor scores of the mines on the first and third PC axes. Plotting these axes resulted in splitting some of the data points, mainly for Colorado mines, from the clusters (Fig. 9B). Since the mines in Colorado operate mostly in thick coal seams with mining heights exceeding 100 inches (2.5 m), they form a separate group scattered between the Alabama mines and the multi-state cluster on the left. However, the West Elk mine is separate from all the groups due to its seam thickness and mining height, 276 inches and 144 inches (7.0 and 3.7 m), respectively, which are high compared to the other mines in the analysis. The Pinnacle No. 50 mine is also separated from the other West Virginia operations and approaches the Virginia mines due to differences in gas contents of the coal seams.

In order to improve interpretability of results, the selected PC matrix (Table 5) was used to create a new component matrix by using Kaiser's varimax rotation method. In varimax rotation, PC axes are rotated to a position in which the sum of the variances of the loadings is the maximum (Grima, 2000). Table 6 shows the rotated matrix for five components (PC_R) and the factor loadings for each variable. This table also shows how the variables are separated between columns according to their characteristics.

Table 6 shows that the first PC_R is mostly related to gas content of the mined coalbed, overburden rank, and the methane emissions. The highest loading is from total gas content (0.962), followed by lost plus desorbed gas (0.949), rank (0.917), and overburden thickness (0.817). Emissions measured from the ventilation system have a loading of 0.646. Selection of a degasification system is a

Table 6
Factor loadings of variables after rotating principal component matrix using Kaiser's varimax rotation

| Variables | PC _R 1 | PC _R 2 | PC _R 3 | PC _R 4 | PC _R 5 |
|----------------------|-------------------|-------------------|-------------------|-------------------|-------------------|
| Basin | -0.296 | 0.010 | -0.137 | 0.907 | -0.133 |
| State | -0.004 | 0.037 | -0.198 | 0.952 | -0.020 |
| Seam height | 0.070 | 0.076 | 0.939 | -0.078 | -0.070 |
| Cut height | 0.054 | -0.036 | 0.917 | -0.211 | -0.067 |
| Panel width | 0.100 | 0.820 | 0.035 | 0.011 | -0.059 |
| Panel length | -0.187 | 0.751 | -0.192 | 0.105 | -0.035 |
| Overburden | 0.817 | -0.083 | 0.112 | -0.124 | 0.131 |
| Number of entries | 0.276 | -0.158 | -0.168 | 0.022 | 0.853 |
| Cut depth | 0.186 | 0.721 | 0.118 | 0.064 | -0.272 |
| Lost+desorbed gas | 0.949 | -0.054 | 0.067 | -0.173 | -0.031 |
| Residual gas | -0.212 | 0.279 | 0.042 | 0.777 | 0.285 |
| Total gas | 0.962 | 0.002 | 0.080 | -0.016 | 0.029 |
| Rank | 0.917 | -0.011 | -0.082 | -0.163 | 0.193 |
| Coal production | -0.173 | 0.755 | 0.121 | 0.213 | 0.061 |
| Ventilation emission | 0.646 | 0.339 | 0.104 | -0.251 | 0.369 |

Bold entries show most influential variables in each rotated principal component (PC_R).

direct consequence of emissions or the capacity of the ventilation system. Thus, it should be included in any model. The second PC_R is weighted by longwall panel dimensions, cut depth, and coal production. In this group, panel width and coal production have the highest loadings (0.820 and 0.755), followed by longwall panel length (0.751) and cut depth (0.721). The third PC_R in Table 6 represents the coalbed and mining heights, where their loadings are 0.939 and 0.917, respectively. The fourth PC_R in Table 6 is related to geographical location of the mine determined by state and coal basin. These are the only variables in the database that may be linked to the impact of underground geology on emissions from overlying strata. Their loadings in this PC_R are 0.952 and 0.907, respectively. However, since a coal basin can be present in more than one state and underground geology may change based on geographical location, the state variable is more localized and seems to be a better identifier for this purpose. The fifth PC_R represents the number of gateroad entries.

4. Development of a classification ANN to identify longwall degasification systems

ANN simulates the human brain with many relatively simple individual processing elements, called *neurons* (Eberhart and Dobbins, 1990). The neuron layers are interconnected in particular structures to receive input and output. One of the most widely used structures is the MLP due to its applicability to general classifications and regressions.

The input–output flow of a network is performed through hidden layers, with the number of hidden layers dependent on the problem (Flood and Kartam, 1994). The number of neurons in the hidden layers needs to be optimized to train the networks effectively (Maier and Dandy, 2000). Using multiple showings (epochs) of the expected outputs, an error is calculated and propagated back to adjust the interconnection weights to minimize the error. Minimizing the mean squared error (MSE) is the goal of the training process. Minimization of error can be done using a gradient descent method where momentum provides the gradient descent with some inertia so that the solution moves towards a global, rather than local, optimum.

Within the hidden layer, the inputs from neurons are multiplied by interconnection weights and summed and processed by a nonlinear transfer function, or axon. Hyperbolic tangent is one of the most widely used axons. In the case of classification, the output for each class with higher probability should be 1 and others should be 0. This function is usually a “softmax” function in the output layer that will scale the outputs between 0 and 1 and will make the higher probability class stronger and the other classes weaker.

Once the training phase is complete, the performance of the network needs to be validated on an independent data set. Cross-validation is a model evaluation method that gives an indication of how well the ANN will do when it is confronted with data it has not yet seen. It is

important that the validation data should not be used as part of training (Maier and Dandy, 2000).

4.1. Preliminary models and the search for effective input parameters for identification of degasification systems

This section presents the results of attempts to find the appropriate input variables for ANN modeling. The strategy was to start with an ANN structure common to all models and to change the input variables to find that model yielding the best results. For this phase, nine different models were tested (Table 7). In all models, the ANN training and network options were the same so that all models and results could be compared.

A two-hidden-layer ANN with 50 and 30 processing elements for the first and second layers, respectively, was constructed to test the model variables in Table 7. The number of nodes in the output layer was four, each corresponding to a degasification scheme, namely no degasification (N), gob vent borehole (G), horizontal boreholes and gob vent boreholes (HG), and vertical, horizontal, and gob vent boreholes (VHG). Hyperbolic tangent was selected as the transfer function for the hidden layers and softmax function was selected for the output layer. A gradient descent search algorithm was utilized with step sizes varying between 1 and 0.01. For all layers, a momentum factor of 0.7 was applied. Training epochs were 1500 in each modeling attempt.

For pre-processing of the input data (exemplars), the dataset was first randomized and then separated into three sections for training, cross-validation, and testing phases. Randomization prevented biases and made subsets of the dataset representative of the whole population. In separating the dataset, 403 out of 538 exemplars (75%) were saved as training data, 54 exemplars (10%) were saved as cross-validation data sets, and 81 exemplars (15%) were saved for testing the trained network.

Table 8 shows the performance data of preliminary input variables (Table 7) in training and cross-validation phases. In order to evaluate the performance of these variables, minimum MSEs were noted for training and

Table 7
Different models and variables tested in ANN

| Model number | Input variables ^a |
|--------------|---|
| 1 | Total gas, Panel W, Entries, State, Seam H. |
| 2 | Total gas, Panel W, Panel L., State, Seam H. |
| 3 | Total gas, Panel W, State, Seam H., Cut H. |
| 4 | Total gas, Panel W, State, Seam H., Rank |
| 5 | Total gas, Panel W, State, Seam H., Cut D. |
| 6 | Total gas, Panel W, Coal P., State, Seam H., Vent E. |
| 7 | Total gas, Panel W, Coal P., State, Seam H., Vent E., Cut H. |
| 8 | Total gas, Panel W, Coal P., State, Seam H., Vent E., Cut H., OB. |
| 9 | Total gas, Panel W, Coal P., State, Seam H., Vent E., Cut H., Entries |

^a OB: overburden; Panel W: panel width; Panel L.: panel length; Seam H.: seam height; Cut H.: cut height; Cut D.: cut depth; Coal P.: coal production; Vent E.: ventilation emission; Entries: number of entries.

Table 8

Training and cross-validation mean squared errors (MSE) for each tested model shown in Table 7

| Model number | Training MSE | Cross-validation MSE |
|--------------|--------------|----------------------|
| 1 | 0.009672 | 0.016827 |
| 2 | 0.007019 | 0.090226 |
| 3 | 0.009130 | 0.017182 |
| 4 | 0.013726 | 0.015097 |
| 5 | 0.008895 | 0.088342 |
| 6 | 0.005677 | 0.011981 |
| 7 | 0.005156 | 0.005666 |
| 8 | 0.004355 | 0.007716 |
| 9 | 0.004455 | 0.012284 |

Table 9

Performance of tested models (in % correct) given in Table 7 in identifying degasification systems included in "testing" data set

| Model number | HG (Horizontal+ GVB) | N (None) | G (GVB) | VHG (Vertical+ Horizontal+ GVB) |
|--------------|----------------------------|-------------|------------|--|
| 1 | 86.4 | 96.9 | 60.0 | 100.0 |
| 2 | 90.9 | 25.0 | 26.7 | 58.3 |
| 3 | 77.3 | 87.5 | 80.5 | 100.0 |
| 4 | 77.3 | 90.6 | 86.7 | 75.0 |
| 5 | 81.8 | 50.0 | 66.7 | 58.3 |
| 6 | 90.9 | 93.8 | 66.7 | 100.0 |
| 7 | 81.8 | 90.6 | 73.3 | 91.7 |
| 8 | 86.4 | 93.8 | 80.0 | 91.7 |
| 9 | 86.4 | 93.8 | 66.7 | 91.7 |

cross-validation. For testing the same models, identification accuracy was noted for the four different degasification schemes (Table 9). The data in Table 8 show that "model 8" produced the least MSE training error (0.004355). The cross-validation error was the second lowest after "model 7." The degasification system in the testing set was more correctly identified using "model 8" than "model 7." Testing of "model 8" produced 86.4%, 93.8%, 80%, and 91.7% correct identifications for HG, N, G, and VHG classes, respectively (Table 9). Thus, the input variables for "model 8," namely, total gas content, panel width, coal production, state, seam height, cut height, overburden thickness, and ventilation emissions were selected as the input variables for the degasification system identification model (Table 7).

4.2. Determination of final network parameters and its identification performance

In order to improve identification performance, the form of the final model was optimized using various combinations of network parameters. For this purpose, two hidden layers were chosen, hyperbolic tangent transfer function was used in the hidden layers, and softmax function was used in the output layer. The number of processing elements in the hidden layers, the value of momentum, and the number of epochs were varied.

The number of processing elements in the first hidden layer was changed between 44 and 58 while maintaining 30 processing elements in the second layer, maintaining the momentum at 0.7, and running the network for 1500 epochs. The results showed that 48 processing elements in the first hidden layer produced the lowest MSEs of 0.003197 and 0.005485 for training and cross-validation, respectively. Next, the number of processing elements in the second hidden layer was varied between 24 and 38, while the number of processing elements in the first hidden layer was set to 48. The minimum MSE was 0.003462 and 0.004766 for training and cross-validation, respectively, with 28 processing elements in the second hidden layer.

Momentum was varied between 0.5 and 0.8 while keeping the number of processing elements in the first and second hidden layers to their optimal values of 48 and 28, respectively. The minimum MSEs of 0.003462 and 0.004766 for training and cross-validation were achieved with a momentum of 0.7. The number of training epochs was varied from 1000 to 2000. For 1000 and 2000 epochs, the cross-validation errors increased to 0.008201 and 0.007087, respectively, as opposed to 0.004766 that was achieved with 1500 epochs. Thus, 1500 was selected as the number of epochs for training and cross-validation.

Based on the performance of the network with different elements, the final network had two hidden layers with 48 and 28 processing elements, hyperbolic

tangent and softmax axon as the transfer functions, a momentum term of 0.7, and a training epoch of 1500. Fig. 10 shows the topology and parameters of the final ANN network used to design the degasification system.

Table 10 shows the performance of the optimized (final) network with testing data set. This table shows the “true” and “false” identifications for each class and the accuracies achieved by the model. As can be seen from this table, the network identified one case out of 22 samples falsely for the HG-type degasification system, for an accuracy of 95%. The model correctly identified 29 mines without any degasification system (N) out of 32 samples. It identified three of them falsely and recommended an “HG” system instead. For gob vent borehole identification (G), out of 15 samples the model identified 12 of them correctly and recommended one of them as HG and two of them as N. The highest score was obtained for the VH system. The ANN identified all 12 cases correctly.

5. Summary and conclusions

The objective of this work was to develop an ANN-based recognition model for identifying the need and type of degasification system for US longwall operations. The variables of the dataset that likely have impact on degasification system selection were analyzed with PCA.

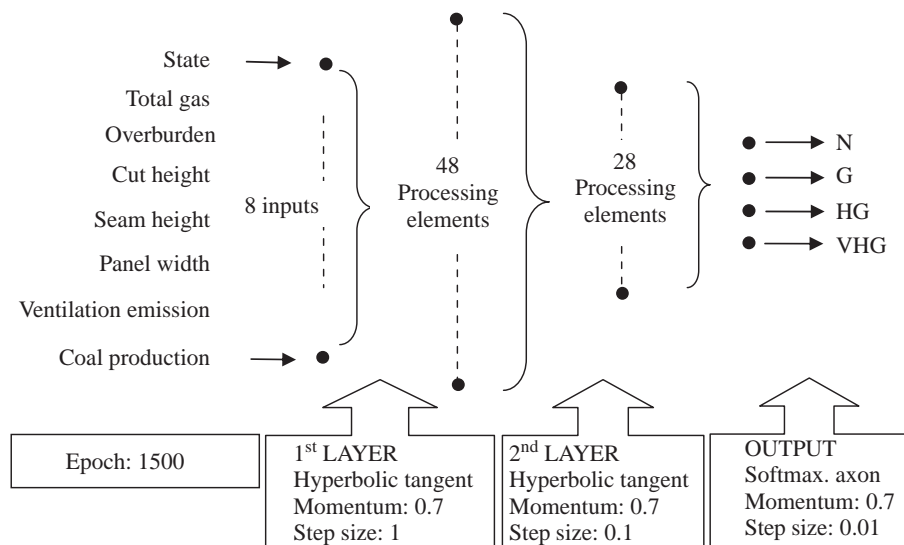


Fig. 10. Inputs, topology, and parameters of proposed ANN model for identification of a suitable degasification system (N: none; G: gob vent boreholes; HG: horizontal boreholes and gob vent boreholes; VH: vertical, horizontal and gob vent ventholes) for US longwall mines.

Table 10
Testing performance of final ANN model (Fig. 10) after optimizing network parameters

| ANN output | HG (Horizontal+GVB) | N (None) | G (GVB) | VHG (Vertical+Horizontal+GVB) |
|------------|------------------------|-------------|------------|----------------------------------|
| HG | 21 (True) | 3 (False) | 1 (False) | 0 |
| N | 0 | 29 (True) | 2 (False) | 0 |
| G | 1 (False) | 0 | 12 (True) | 0 |
| VHG | 0 | 0 | 0 | 12 (True) |
| % Correct | 95.5 | 90.6 | 80.0 | 100.0 |

Based on the results, a number of models were tested to find the best combination of variables for selecting a degasification system using the ANN approach. Finally, the parameters of the ANN were optimized to improve the classification performance of the model. The final model had two hidden layers with 48 and 28 processing elements in each layer.

Results showed that degasification systems that are commonly used at US longwall mines can be classified effectively using a few variables. This study showed that using the variables of state, total gas content of coalbed, seam and cut heights, panel width, coal productions, overburden depths of the mines, and ventilation emissions resulted in high accuracies for correctly identifying the use of no degasification, gob vent boreholes (GVB), horizontal and GVB, and horizontal, vertical, and GVB designs.

The approach and the results suggest that, by incorporating the critical stratigraphic features in place of geographical information, this model can be applicable to other mines in different locations. This model can also be used as a screening tool prior to applying more detailed simulation studies for optimizing recovery efficiencies of the ANN-identified systems.

Acknowledgment

Barbora Jemelkova of the EPA is thanked for her help in obtaining ventilation methane emission data. W.P. Diamond is thanked for his help in obtaining gas content data.

References

- An, P., Chung, C.F., Rencz, A.N., 1995. Digital lithology mapping from airborne geophysical and remote sensing data in the Melville Peninsula, Northern Canada, using a neural network approach. *Remote Sensing of Environment* 53, 76–84.
- Brown, D.G., Lusch, D.P., Duda, K.A., 1998. Supervised classification of types of glaciated landscapes using digital elevation data. *Geomorphology* 21, 233–250.
- Brunner, D.J., Schwoebel, J.J., Li, J., 1997. Simulation based degasification system design for the Shihao mine of the Songzao Coal Mining Administration in Sichuan China. In: *Proceedings of the 6th International Mine Ventilation Congress*, Pittsburgh, PA, pp. 429–433.
- Chen, D.R., Chang, R.F., Kuo, C.W.J., Chen, M.C., Huang, Y.U.L., 2002. Diagnosis of breast tumors with sonographic texture analysis using wavelet transform and neural networks. *Ultrasound in Medicine and Biology* 28, 1301–1310.
- Diamond, W.P., 1994. Methane Control for Underground Coal Mines. US Bureau of Mines Information Circular No. 9395, Pittsburgh, PA, (44pp.).
- Diamond, W.P., Schatzel, S.J., 1998. Measuring the gas content of coal: a review. *International Journal of Coal Geology* 35, 311–331.
- Diamond, W.P., La Scola, J.C., Hyman, D.M., 1986. Results of Direct-Method Determination of the Gas Content of the US Coalbeds. US Bureau of Mines Information Circular No. 9067, Pittsburgh, PA, (95pp.).
- Diamond, W.P., Boddien, W.R., Zuber, M.D., Schraufnagel, R.A., 1989. Measuring the extent of coalbed gas drainage after 10 years of production at the Oak Grove Pattern, Alabama. In: *Proceedings of the 1989 Coalbed Methane Symposium*, Tuscaloosa, AL, pp. 185–193.
- Eberhart, R.C., Dobbins, R.W., 1990. *Neural Network PC Tools: A Practical Guide*, first ed. Academic Press, San Diego, CA, (275pp.).
- EPA, 1994. Identifying opportunities for methane recovery at US coal mines: draft profiles of selected gassy underground coal mines. US Environmental Protection Agency Report No. EPA-430-R-94-012, Washington, DC, 212pp.
- EPA, 2005. Identifying opportunities for methane recovery at US coal mines: profiles of selected gassy underground coal mines 1999–2003. US Environmental Protection Agency Report No. EPA-430-K-04-003, Washington, DC, 202pp.
- Flood, I., Kartam, N., 1994. Neural networks in civil engineering. I: Principles and understanding. *Journal of Computing in Civil Engineering* 8, 131–148.
- Grima, M.A., 2000. *Neuro-Fuzzy Modeling in Engineering Geology*. A.A. Balkema, Rotterdam, Netherlands, (244pp.).
- Hong, Y.S.T., Rosen, M.R., Bhamidimarri, R., 2003. Analysis of a municipal wastewater treatment plant using a neural network-based pattern analysis. *Water Research* 37, 1608–1618.
- Karacan, C.Ö., 2008. Development and application of reservoir models and artificial neural networks for optimizing ventilation air requirements in development mining of coal seams. *International Journal of Coal Geology* 73, 371–387.
- Karacan, C.Ö., Diamond, W.P., 2006. Forecasting gas emissions for coal mine safety applications. In: Kissell, F. (Ed.), *Handbook for Methane Control in Mining*. National Institute for Occupational Safety and Health Information Circular No. 9486, Pittsburgh, PA, pp. 113–126.
- Karacan, C.Ö., Diamond, W.P., Esterhuizen, G.S., Schatzel, S.J., 2005. Numerical analysis of the impact of longwall panel width on methane emissions and performance of gob gas ventholes. In: *Proceedings of the 2005 International Coalbed Methane Symposium*, Paper No. 0505, Tuscaloosa, Alabama.
- Karacan, C.Ö., Diamond, W.P., Schatzel, S.J., 2007a. Numerical analysis of the influence of in-seam horizontal methane drainage boreholes on longwall face emission rates. *International Journal of Coal Geology* 72, 15–32.
- Karacan, C.Ö., Esterhuizen, G.S., Schatzel, S.J., Diamond, W.P., 2007b. Reservoir simulation-based modeling for characterizing longwall methane emissions and gob gas venthole production. *International Journal of Coal Geology* 71, 225–245.
- Kelafant, J.R., Boyer, C.M., Zuber, M.D., 1988. Production potential and strategies in the Central Appalachian Basin. In: *Proceedings of the Society of Petroleum Engineers Eastern Regional Meeting*, Charleston, WV, pp. 305–312.
- Kılıç, K., Boyacı, I.H., Köksel, H., Küsmenoğlu, I., 2007. A classification system for beans using computer vision system and artificial neural networks. *Journal of Food Engineering* 78, 897–904.
- Kim, A.G., 1977. Estimating Methane Content of the Bituminous Coalbeds from Adsorption Data. US Bureau of Mines Report of Investigations No. 8245, Pittsburgh, PA, (22pp.).
- King, G.R., Ertekin, T., 1989. State-of-the-art in modeling of unconventional gas recovery. In: *Proceedings of the 1989 Society of Petroleum Engineers Low Permeability Reservoirs Symposium and Exhibition*, Denver, CO, pp. 173–191.
- King, G.R., Ertekin, T., Schwerer, F.C., 1986. Numerical simulation of the transient behavior of coal-seam degasification wells. *SPE (Society of Petroleum Engineers) Formation Evaluation* 1 (2), 165–183.
- Maier, H.R., Dandy, G.C., 2000. Neural networks for the prediction and forecasting of water resources variables: a review of modeling issues and applications. *Environmental Modeling and Software* 15, 101–124.
- Mucho, T.P., Diamond, W.P., Garcia, F., Byars, J.D., Cario, S.L., 2000. Implications of recent NIOSH tracer gas studies on bleeder and gob gas ventilation design. In: *Proceedings of the Society of Mining Engineers, Annual Meeting*, Salt Lake City, UT, pp. 1–17.
- Noack, K., 1998. Control of gas emissions in underground coal mines. *International Journal of Coal Geology* 35, 57–82.
- Pashin, J., 1998. Stratigraphy and structure of coalbed methane reservoirs in the United States: an overview. *International Journal of Coal Geology* 35, 209–240.
- Peng, S.S., 2006. *Longwall Mining*, second ed. West Virginia University Press, Morgantown, WV, (621pp.).
- Remner, D.J., Ertekin, T., Sung, W., King, G.R., 1986. A parametric study of the effects of coal seam properties on gas drainage efficiency. *SPE (Society of Petroleum Engineers) Reservoir Engineering* 1 (6), 633–645.
- Steidl, P., 1996. Coal as a reservoir. In: Saulsbury, J.L., Scahfer, P.S., Schraufnagel, R.A. (Eds.), *Coalbed Methane Reservoir Engineering*. Gas Research Institute, Chicago, IL, pp. 30–46.
- Thakur, P.C., 2006. Coal seam degasification. In: Kissell, F. (Ed.), *Handbook for Methane Control in Mining*. National Institute for Occupational Safety and Health Information Circular No. 9486, Pittsburgh, PA, pp. 77–96.